AFRL-RY-WP-TP-2010-1244

ANALYSIS AND CHARACTERIZATION OF THE SMALL-SIGNAL MODULATION OF A VERTICAL EXTERNAL CAVITY SURFACE EMITTING LASER (POSTPRINT)

N. Terry, M. Walton, and Robert Bedford

Electro Optic Components Branch
Aerospace Components and Subsystems Technology Division

FEBRUARY 2010

AIR FORCE RESEARCH LABORATORY
SENSORS DIRECTORATE
WRIGHT-PATTERSON AIR FORCE BASE, OH 45433-7320
AIR FORCE MATERIEL COMMAND
UNITED STATES AIR FORCE

REPORT DOCUMENTATION PAGE

Form Approved
OMB No. 0704-0188

1. REPORT DATE *(DD-MM-YY)*	2. REPORT TYPE	3. DATES COVERED *(From - To)*
February 2010	Conference Paper Postprint	01 January 2009 – 01 September 2009

4. TITLE AND SUBTITLE
ANALYSIS AND CHARACTERIZATION OF THE SMALL-SIGNAL MODULATION OF A VERTICAL EXTERNAL CAVITY SURFACE EMITTING LASER (POSTPRINT)

5a. CONTRACT NUMBER
In-house

5b. GRANT NUMBER

5c. PROGRAM ELEMENT NUMBER
62204F

6. AUTHOR(S)
N. Terry, M. Walton, and Robert Bedford

5d. PROJECT NUMBER
2002

5e. TASK NUMBER
IH

5f. WORK UNIT NUMBER
2002IH0E

7. PERFORMING ORGANIZATION NAME(S) AND ADDRESS(ES)
Electro Optic Components Branch (AFRL/RYDP)
Aerospace Components and Subsystems Technology Division
Air Force Research Laboratory, Sensors Directorate
Wright-Patterson Air Force Base, OH 45433-7320
Air Force Materiel Command, United States Air Force

8. PERFORMING ORGANIZATION REPORT NUMBER
AFRL-RY-WP-TP-2010-1244

9. SPONSORING/MONITORING AGENCY NAME(S) AND ADDRESS(ES)
Air Force Research Laboratory
Sensors Directorate
Wright-Patterson Air Force Base, OH 45433-7320
Air Force Materiel Command
United States Air Force

10. SPONSORING/MONITORING AGENCY ACRONYM(S)
AFRL/RYDP

11. SPONSORING/MONITORING AGENCY REPORT NUMBER(S)
AFRL-RY-WP-TP-2010-1244

12. DISTRIBUTION/AVAILABILITY STATEMENT
Approved for public release; distribution unlimited.

13. SUPPLEMENTARY NOTES
Conference paper published in the *Proceedings of the Physics and Simulation of Optoelectronic Devices XVIII*, conference held 25 January 2010 in San Francisco, California. PAO Case Number: 88ABW-09-5316; Clearance Date: 10 Jan 2010. Paper contains color.

14. ABSTRACT
The small signal modulation of a vertical external cavity surface emitting laser (VECSEL) is examined. The modulation transfer function (MTF) of the cavity is measured for multiple photon lifetimes operating between Class A and Class B regimes, where the photon and carrier lifetimes are of the same order. Three coupled ordinary differential equations with similarities to an electrically-injected quantum-well laser with a separate confinement heterostructure are used to mathematically describe the time-dependant VECSEL response. We present a series of measurements that provide important laser parameters such as internal device losses and differential gain. The VECSEL operating in this regime is an overdamped oscillator and has free-running characteristics that are not unlike quantum-dot and quantum-cascade lasers.

15. SUBJECT TERMS
lasers, semiconductor

16. SECURITY CLASSIFICATION OF:			17. LIMITATION OF ABSTRACT:	18. NUMBER OF PAGES	19a. NAME OF RESPONSIBLE PERSON (Monitor)
a. REPORT	b. ABSTRACT	c. THIS PAGE			Robert Bedford
Unclassified	Unclassified	Unclassified	SAR	16	19b. TELEPHONE NUMBER *(Include Area Code)* N/A

Standard Form 298 (Rev. 8-98)
Prescribed by ANSI Std. Z39-18

Analysis and characterization of the small-signal modulation of a vertical external cavity surface emitting laser

N. Terry , M. Walton, R. Bedford

Air Force Research Laboratory, Wright Patterson AFB, OH 45433-7321

ABSTRACT

The small signal modulation of a vertical external cavity surface emitting laser (VECSEL) is examined. The modulation transfer function (MTF) of the cavity is measured for multiple photon lifetimes operating between Class A and Class B regimes, where the photon and carrier lifetimes are of the same order. Three coupled ordinary differential equations with similarities to an electrically-injected quantum-well laser with a separate confinement heterostructure are used to mathematically describe the time-dependant VECSEL response. We present a series of measurements that provide important laser parameters such as internal device losses and differential gain. The VECSEL operating in this regime is an overdamped oscillator and has free-running characteristics that are not unlike quantum-dot and quantum-cascade lasers.

Keywords: semiconductor laser, diode-pumped lasers, modulation, relaxation oscillations, VECSEL

1. INTRODUCTION

Semiconductor lasers are increasingly popular bright optical sources, due primarily to the advent of the vertical external cavity surface emitting laser (VECSEL),[1–4] also known as the optically pumped semiconductor laser. These lasers have been effective at wavelengths ranging from visible[5] to short-wave infrared[6] using direct semiconductor lasing. Due to the "open" nature of the cavity, nonlinear crystals may also be incorporated to efficiently convert from the ultraviolet through upconversion via second-harmonic generation[7] to short-wave infrared through an intracavity optical parametric oscillator.[8] Other nonlinear components may also be inserted into the cavity, for example saturable absorbers for mode-locking.[9]

From a dynamics point of view, VECSELs are potentially interesting because the photon lifetime and carrier lifetime can be widely varied, from regimes where they are the same order of magnitude, to regimes where the two lifetimes differ by several orders of magnitude. This differs from traditional semiconductor lasers (both edge- and surface-emitting), where the photon lifetime is approximately three orders of magnitude smaller than the carrier lifetime, identified as Class-B lasers. Class-A lasers (where the photon lifetime is much longer than the carrier lifetime) are found at the other limit of operation. VECSELs therefore are tunable from weakly Class-B through to Class-A operation, an unusual attribute of most lasers.

In this paper, we study the small signal modulation of a VECSEL. The small signal regime is useful because it allows us to apply simplifying assumptions to the rate equations. These simplifications result in a simple analytic formula which describes the output of the laser as a function of the frequency modulation of the input. A simplified formula can be used to fit the data and extract important operational laser parameters like the resonance frequency, the damping and carrier lifetime. A further analysis of the rate equations allows the extraction the differential gain, scattering and absorption losses, as well as the transparency carrier density, the shift carrier density and the material gain of the active region. All of these parameters can be determined through non-destructive examination of the laser, making the small signal regime a useful analytical framework for describing the VECSEL system and its components.

Further author information: (Send correspondence to N.T..)
N.T.: E-mail: nathan.terry@wpafb.af.mil, Telephone: 1 937 904 9973

Physics and Simulation of Optoelectronic Devices XVIII, edited by
Bernd Witzigmann, Fritz Henneberger, Yasuhiko Arakawa, Marek Osinski, Proc. of SPIE
Vol. 7597, 75972B · © 2010 SPIE · CCC code: 0277-786X/10/$18 · doi: 10.1117/12.852283

2. THEORY

The basic theory of the VECSEL considers the interaction of the carriers in the quantum well with the carriers in the barrier and with the photons in the cavity. These equations are similar to that of SCH lasers, except there are pump terms in both the barrier and well carrier equations. The interplay between these three quantities can be described with the following coupled differential laser rate equations:

$$\frac{d}{dt}N_w = \frac{P_i}{V_w\hbar\omega_p}\Omega_w - R_w - \frac{N_w}{\tau_{bw}} + \frac{L_b}{L_w}\frac{N_b}{\tau_{wb}} - v_g\Gamma_R g_w N_p \quad (1)$$

$$\frac{d}{dt}N_b = \frac{P_i}{V_b\hbar\omega_p}\Omega_b - R_b + \frac{L_w}{L_b}\frac{N_w}{\tau_{bw}} - \frac{N_b}{\tau_{wb}} \quad (2)$$

$$\frac{d}{dt}N_p = -\frac{N_p}{\tau_p} + v_g\Gamma_R\Gamma g_w N_p + \beta_{sp}\Gamma B_w N_w^2 \quad (3)$$

$$g_w = \frac{g_\circ}{1+\epsilon N_p}\log\left(\frac{N_w+N_s}{N_{tr}+N_s}\right) \quad (4)$$

N_w represents the carrier density in the quantum wells, N_b is the carrier density in the barrier region and N_p the photon density. P_i is the pump power, $\Omega_{w,b}$ is the absorption efficiency at the pump frequency ω_p, $V_{w,b}$ is the volume, $R_{w,b}$ is the carrier loss rates and includes non-radiative recombination, spontaneous emission and Auger recombination. The subscript of each of these terms describes whether the term applies to the wells or the barriers. The terms τ_{wb} and τ_{bw} are respectively the lifetime of the transition of the carriers from the barrier to the well and vice-versa. The photon lifetime is represented by τ_p, v_g is the group velocity in the gain region, and Γ_R is the resonant gain enhancement. We chose to represent the gain (g_w) using a logarithmic gain-carrier relation, where the transparency current density is represented by N_{tr} and N_s represents the shift carrier density. β_{sp} is the spontaneous emission term, and Γ is the 3-dimensional overlap integral.

3. EXPERIMENTAL SETUP

3.1. Active gain region

The cavity is an epitaxially grown mirror/active region and an external curved mirror supporting a stable mode. The active region consists of 14 strained InGaAs quantum-wells in a resonant periodic gain configuration with strain compensating layers designed to operate at approximately 976 nm at 20 °C. The active region is heterogeneously grown with a distributed Bragg reflector and comprises one mirror of the resonator. Fabrication entails solder bonding the chip to a diamond heat spreader, removing the substrate, and applying a low reflectance single-layer dielectric coating onto the surface, significantly reducing both pump and lasing reflections from the semiconductor/air interface. Further details of this structure and its cw performance can be found elsewhere.[10]

3.2. Laser cavity

The setup is shown in Fig. 1. A 200 mm radius of curvature output coupler is placed 3 cm from the gain region. The cavity is allowed to run in multiple transverse and longitudinal modes without intracavity filtering elements. The VECSEL chip is pumped with two 808 nm lasers. First, a high-power fiber-coupled laser bar imaged onto the semiconductor surface at an angle of approximately 40-degrees results in a pump ellipse with a minor axis of 200 μm, herein referred to as "bias pump." This laser provides a time-independent value for P_i in Equations 1 and 2. For the modulation tests, a second, lower power ridge laser at nominally the same wavelength is biased above threshold and is sinusoidally modulated with an RMS optical amplitude of approximately 18 μW. This second ac pump is imaged onto the chip surface and overlaps an area slightly smaller than the bias pump to allow for high speed controllable small-signal modulation.

The electrical input to the ac pump is adjusted to compensate for the MTF response of the ridge laser, thus maintaining constant output optical amplitude independent of modulation frequency. This explicitly isolates the response of the VECSEL for the purposes of characterizing the laser itself. The combination of these two pumps allows for biasing the VECSEL above threshold and modulating small amplitudes above this bias point,

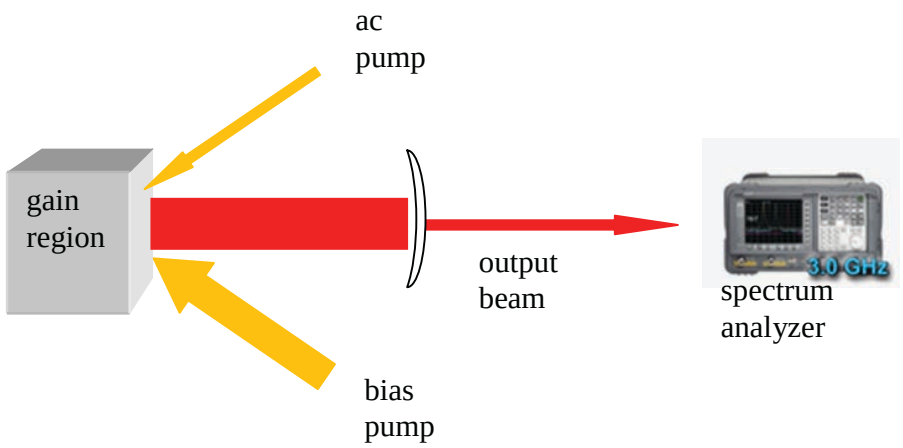

Figure 1. A diagram of the experimental setup. The optical cavity consisted of an active gain region and a 200 mm radius of curvature output coupler. The cavity is optically pumped with two lasers. One pump laser operates at a fixed bias pump power; modulation is introduced via the ac pump laser. The VECSEL output is fiber coupled into a spectrum analyzer which is used to measure the modulation transfer function.

and is not dissimilar to direct-drive modulation of electrically injected lasers. The bias power out of the cavity is maintained at 1 W or less to minimize thermal loading, which is ignored in the model. Output from the VECSEL is characterized using a pyrometer for measuring the bias output power; the output was also characterized by using a high-speed detector connected to an rf spectrum analyzer.[11]

Due to the versatility of the VECSEL, there are multiple ways to adjust the photon lifetime, given by:

$$\frac{1}{\tau_p} = \frac{1}{2}\left(\frac{cv_g}{v_g L_p + cL_a}\right)\left[\ln\left(\frac{1}{R_1 R_2}\right) + \ln\left(\frac{1}{S^2}\right)\right] \tag{5}$$

where c and v_g are the speed of light in the passive region and group velocity in the active region, respectively. The lengths of the active and passive regions are given by L_a and L_p, respectively, while the mirror reflectivity is given by R_1 and R_2. The distributed Bragg reflector (DBR) has a calculated reflectance greater than 0.999; our outcoupler reflectance (R_2) was varied. Finally, losses within a round trip are dominated by scattering at the semiconductor-air interface, which is accounted for by S. To change the photon lifetime, it is straight forward to simply adjust the passive cavity length (distance between the chip and the output coupler), however in this linear cavity, this also changes the mode size on the semiconductor and therefore changes in Equation 3. Rather, we chose to vary the reflectance of the output coupler, which leaves the mode overlap identical. We used four output couplers which we have measured the reflectances to be 0.959, 0.983, 0.99, and 0.995. These correspond to photon lifetimes of 3.51 ns, 6.37 ns, 7.66 ns, and 12.08 ns, respectively. The carrier lifetime (a value nominally R_w/N_w) is on the order of 5 ns, therefore we are investigating the border region between Class-A and Class-B lasers.

4. RESULTS AND DISCUSSION

An analysis of the steady-state (cw) output from the VECSEL provides insight into some of the terms in Equations 1-4. Ignoring spontaneous emission, Equations 1-3 show the output power of the VECSEL (P_o) above threshold is related to the input power and the recombination losses of the system according to:

$$P_o = Z\Omega\Gamma_T\Delta_p P_i - Z\hbar\omega_l\Gamma_T\left(V_w R_w + V_b R_b\right) \tag{6}$$

where ω_l is the output frequency of the VECSEL and Γ_T is the transverse mode overlap of the input pump modes. The output power as a function of bias pump input power for the various cavity configurations is shown

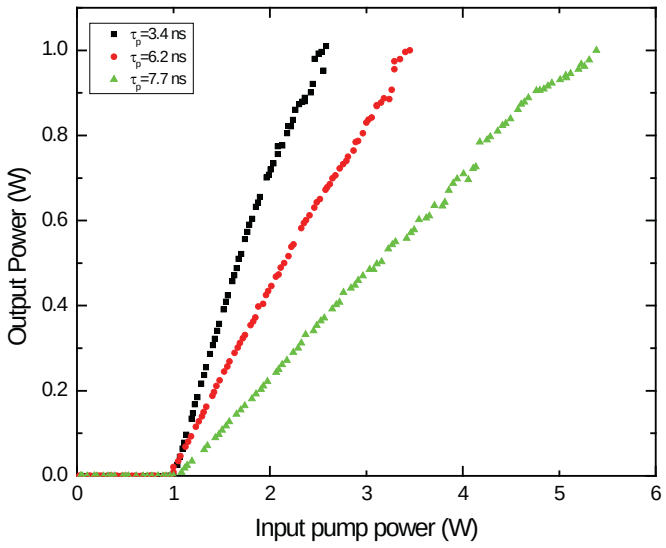

Figure 2. The output of the VECSEL as a function of pump power for 3 different cavity configurations. The output coupler of each cavity had a unique reflectivity and photon lifetime.

in Figure 2 The difference in pump photon and lasing photon energies is given by the quantum defect, Δ_p, while Ω is the total absorption of the pump light by the semiconductor chip. The term Z accounts for the fact that not all the optical losses of the cavity are due the output coupler; optical scattering losses are also a consideration. This is especially important in the case of higher reflectivity mirrors, where the fraction of light that is lost to scattering may be of similar magnitude to light that is transmitted through the outcoupler. The Z term takes this into account by noting that the useful output power of the VECSEL is proportional to the ratio of the mirror losses to the total losses:

$$Z = \frac{\log\left(R_2^{-1}\right)}{\log\left(R_1^{-1}R_2^{-1}\right) + \log\left(S^{-1}\right)}. \tag{7}$$

4.1. Determining the internal scattering losses and absorption

In this analysis, we first look at the slope efficiency, the derivative of Equation 6:

$$\frac{\partial P_o}{\partial P_i} = Z\Omega\Gamma_T\Delta_p \tag{8}$$

In this equation, we can calculate the photon defect because the pump and lasing wavelengths are known. The transverse mode confinement may also be calculated through the pump size and the known sizes of the Hermite-Gaussian modes on the active region. This leaves us with an absorption constant (Ω) and Z. The scattering losses and the absorption in the active region can be determined by measuring the slope efficiency for several cavity configurations with different output couplers. As we look at the slope efficiency (plotted in Fig. 3a) as a function of mirror reflectance and fit this with Equation 8 as a function of mirror reflectance, we extracted the absorption constant as well as the scattering loss; an excellent fit of Equation 8 to the data was obtained for a scattering value of S=0.992 and an absorption of Ω=0.655. We should note that this scattering term is somewhat smaller than a typical value one would desire to use in a high-efficiency laser, where we would hope S >0.995. This method is analogous to the cutback method for characterizing semiconductor and fiber lasers, because although we are not adjusting the internal loss term, we are adjusting the mirror loss. This is an interesting capability for these lasers because unlike the cutback method, this method is non-destructive for these lasers, allowing us to measure the same laser that may undergo further analysis (such as small-signal modulation).

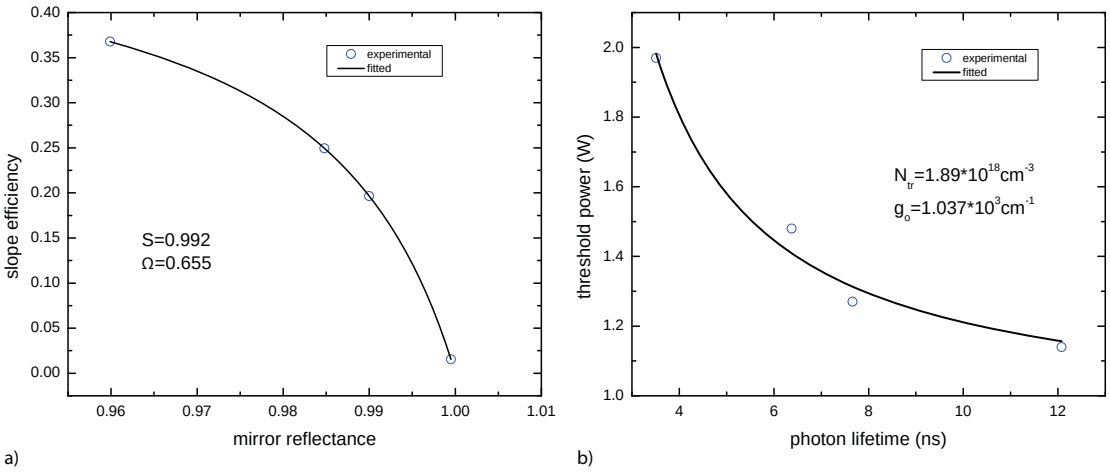

Figure 3. a)The scattering losses and the absorption of the gain region can be determined by measuring the slope efficiency for cavity configurations with different output couplers. These two values are determined by using them as fitting parameters in Equation 8. b) By fitting the experimentally measured relationship between the threshold pump power and the photon lifetime of each cavity configuration with the equations presented in Section 4.2, we determined the transparent carrier density, the shift carrier density and the gain coefficient of the VECSEL.

4.2. Determining the internal scattering losses and absorption

We may rewrite Equation 6, taking the limit that P_o is zero, to represent the threshold power:

$$P_{th} = \frac{\hbar\omega_p}{\Omega}\left(V_w R_w + V_b R_b\right). \tag{9}$$

The transparent current density, the gain coefficient and the shift carrier density can be determined using Equation 4, provided the steady state gain g_w and the threshold carrier density N_w are known. We can determine the threshold carrier density by using Equation 6. The threshold condition can be realized by recalling that the recombination losses are of the form, $R_{w,b} \equiv A_{w,b}N_{w,b} + B_{w,b}N_{w,b}^2 + C_{w,b}N_{w,b}^3$, where A represents non-radiative recombination, B represents radiative recombination and C represents Auger recombination for each of the wells and barriers, as denoted by the subscripts. We may safely ignore the barrier contribution R_b, as the barrier lifetime is sufficiently large, even though V_b is much larger than V_w, because N_b remains small compared to N_w. Assuming that these values are known for the material of interest, it is a simple matter to determine the threshold carrier density N_w, as a function of τ_p. Furthermore, with the values of S found from fitting the slope, we may determine the explicit relation between output coupler reflectance and photon lifetime. The steady state gain can be determined through Equation 3. If we ignore the contribution of spontaneous emission (β_{sp}=0), we can use Equation 3 to solve for the steady state gain, g_w. The data and the associated fits are shown in Figure 3b. This fit varies somewhat from the data, which may be due to poor choices in A, B, and C, or more seriously, may indicate either the power series for the carrier loss term is an inappropriate approximate, or that the gain-carrier relation varies from the logarithmic relation.[12]

4.3. Using the steady-state values to baseline computations

We may use the values determined in Sections 4.1 and 4.2 to show that our modeling accurately predicts the power characteristics in steady-state. Figure 4 shows the numerical data along with experimental data using values of S, Ω, and the gain-carrier relation previously determined.

Though the slope agreement is outstanding, there is a disagreement in threshold. Due to the simplicity of the model along with the potential that the carrier loss terms are limited in applicability, the agreement between theory and experiment is reasonable.

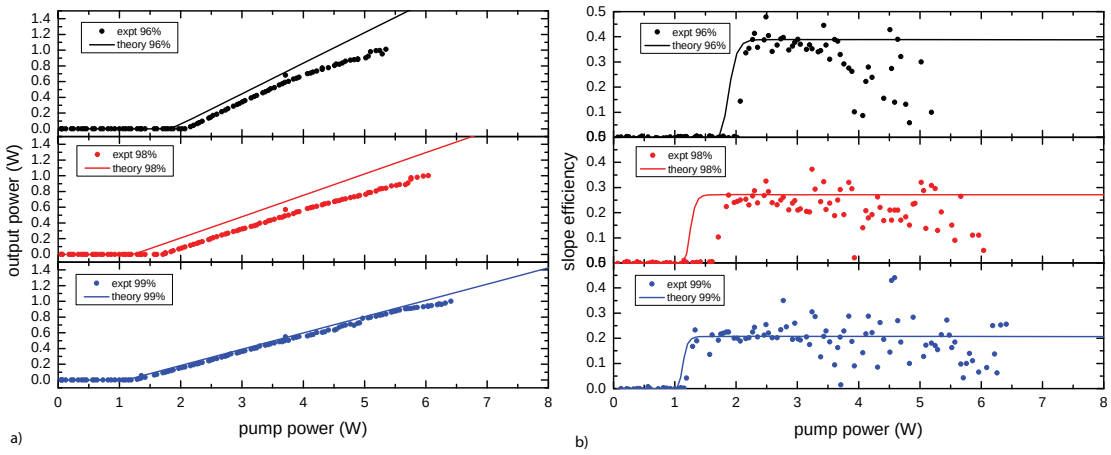

Figure 4. Simulated and experimentally determined data. a) Power curve of the VECSEL for various out-coupler reflectances. Circle data are measured values, while solid lines are simulated steady state values, and essentially equivalent (at least above threshold) to the algebraic line of Equation 6 b) The derivative of (a), showing good agreement near threshold, but a fall off at higher powers because the numerical solutions ignore temperature, an important feature as pump power density increases.

Table 1. Matrix terms used to derive the exact analytical solution

coefficient	function
γ_{ww}	$\frac{1}{\tau_w} + \frac{1}{\tau_{bw}} + v_g \Gamma_R a N_{p0}$
γ_{wb}	$-\frac{L_b}{L_w}\frac{1}{\tau_{wb}}$
γ_{ws}	$v_g \Gamma_R G_0 + v_g \Gamma_R a_p N_{p0}$
γ_{bw}	$-\frac{L_w}{L_b}\frac{1}{\tau_{bw}}$
γ_{bb}	$\frac{1}{\tau_b} + \frac{1}{\tau_{wb}}$
γ_{sw}	$-v_g \Gamma_R \Gamma a N_{p0} - 2\beta_{sp}\Gamma B_w N_{w0}$
γ_{ss}	$\frac{1}{\tau_p} - v_g \Gamma_R \Gamma G_0 - v_g \Gamma_R \Gamma a_p N_{p0}$

4.4. Determining resonance frequency, damping factor

We can use Equations 1-4 and perturb the system's N_w, N_b, N_p, P_i and g_w with a first order Taylor expansion. Using the Cauchy formalism, we may arrive at an exact analytical solution:

$$MTF(\omega) = \left(\frac{\gamma_{ww}\gamma_{ss} - \gamma_{sw}\gamma_{ws} - \frac{\gamma_{wb}\gamma_{bw}\gamma_{ss}}{\gamma_{bb}}}{1 + i\omega/\gamma_{bb}}\right)\left(\frac{1}{\gamma_{wb}\frac{\Omega_b}{V_b} - \gamma_{bb}\frac{\Omega_w}{V_w}}\right) \times \left[\frac{\gamma_{wb}\frac{\Omega_b}{V_b} - \gamma_{bb}\frac{\Omega_w}{V_w} - i\frac{\Omega_w}{V_w}\omega}{\gamma_{ww}\gamma_{ss} - \gamma_{sw}\gamma_{ws} - \frac{\gamma_{wb}\gamma_{bw}\gamma_{ss}}{\gamma_{bb}+i\omega} - \omega^2 + i\left(\gamma_{ww} + \gamma_{ss} - \frac{\gamma_{wb}\gamma_{bw}}{\gamma_{bb}+i\omega}\right)\omega}\right] \quad (10)$$

where the γ_{nm} terms represent the n element being acted upon by the m element. These elements are explicitly given in Table 1. The first term's frequency dependence in Equation 10 is dominated by $1/\gamma_{bb}$, a value that is essentially proportional to the barrier to well scattering rate. The second element in Equation 10 is a constant resulting from the normalization procedure. The third term is not dissimilar to the traditional damped driven harmonic oscillator with extra frequency terms in the coefficients. Above threshold, it is typically acceptable to ignore spontaneous emission as we did to arrive at Equation 6; this simplifies Equation 10 by removing the second term from γ_{sw} and forces γ_{ss} to become zero. This approximation creates a very good approximation to

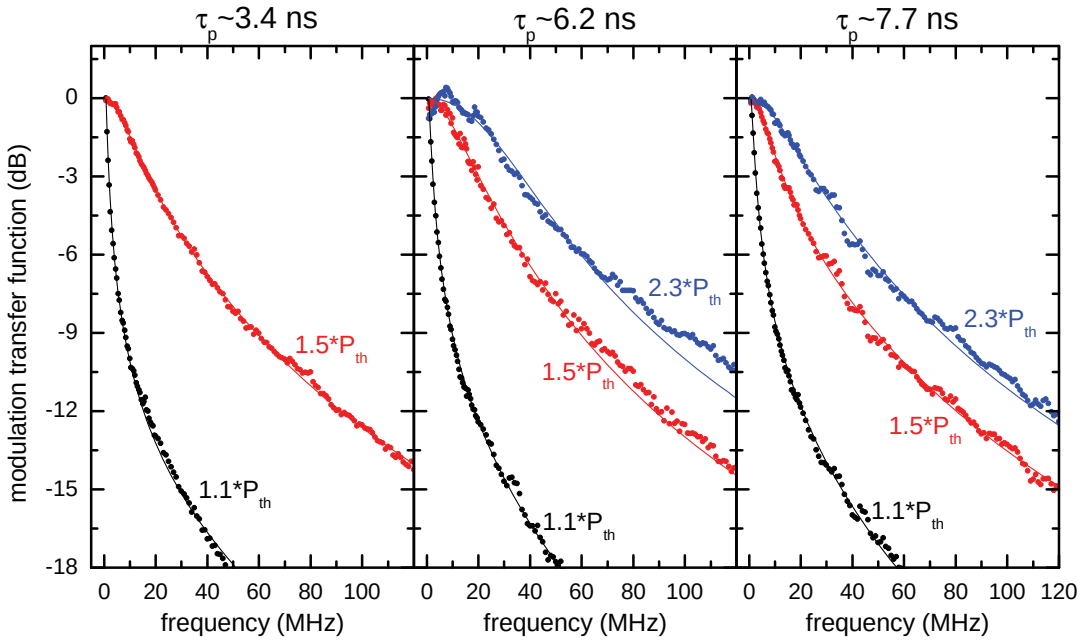

Figure 5. A comparison performance various cavity configurations which presents the MTF for similar pump biases relative to the threshold pump power.

the exact analytical solution:

$$MTF(\omega) \approx \left(1 - i\frac{\omega}{\gamma_r - \gamma_{bb}}\right)\left(\frac{1}{1 + i\omega/\gamma_{bb}}\right)\frac{\omega_r^2}{\omega_r^2 - \omega^2 + i\gamma(\omega)\omega}, \tag{11}$$

where:

$$\begin{aligned} \omega_r^2 &= -\gamma_{sw}\gamma_{ws} \\ \gamma(\omega) &= \left[\gamma_{ww} - \frac{1}{\gamma_{bb}}\left(\frac{\gamma_{wb}\gamma_{bw}}{1 + i\omega/\gamma_{bb}}\right)\right] \\ \gamma_r &= \gamma_{wb}\frac{\Omega_b/V_b}{\Omega_w/V_w} \end{aligned}$$

For typical VECSEL parameters, the first term of Equation 11 remains close to unity. The damping term remains essentially constant as well, for typical VECSEL values. With the added approximation that $1/\gamma_{bb} \sim \tau_{wb}$, we may simplify Equation 11 to a standard 3-pole modulation response.[13] The output power as a function of frequency is given by

$$|MTF(\omega)|^2 \approx \left|\left(\frac{1}{1 + i\tau_{wb}\omega}\right)\left(\frac{\omega_r^2}{\omega_r^2 - \omega^2 + i\gamma\omega}\right)\right|^2, \tag{12}$$

where again ω is the modulation frequency, ω_r is the resonance frequency, γ is the damping factor and τ_{wb} is the relaxation time of carriers from the barrier to the well.

The MTF and the resultant fit at various VECSEL output powers are shown in Figure 5. Each of these fits provided values for the resonance frequency, the damping factor and the carrier lifetime for the output power and corresponding configurations of the VECSEL. The resonance frequencies and the damping factor associated with each of these fits are presented in Table 2.

It should be noted that while the data can be fitted with the 3-pole model of Equation 12, it is also possible to fit the data using the standard two pole model which neglects the relaxation time of the carriers from the

Table 2. The resonance frequency (ω_r), damping (γ) and the differential gain (a) were extracted by fitting the MTF data to Equation 12. This data was determined for 300mW of output power (P_o).

τ_p (ns)	3.4	6.2	7.7
$\omega_r/2\pi$ (MHz)	21.3	23.3	29.8
$\gamma/2\pi$ (MHz)	51.7	53.8	71.1
a (cm^2)	$8.5 * 10^{-16}$	$8.87 * 10^{-16}$	$1.2 * 10^{-15}$

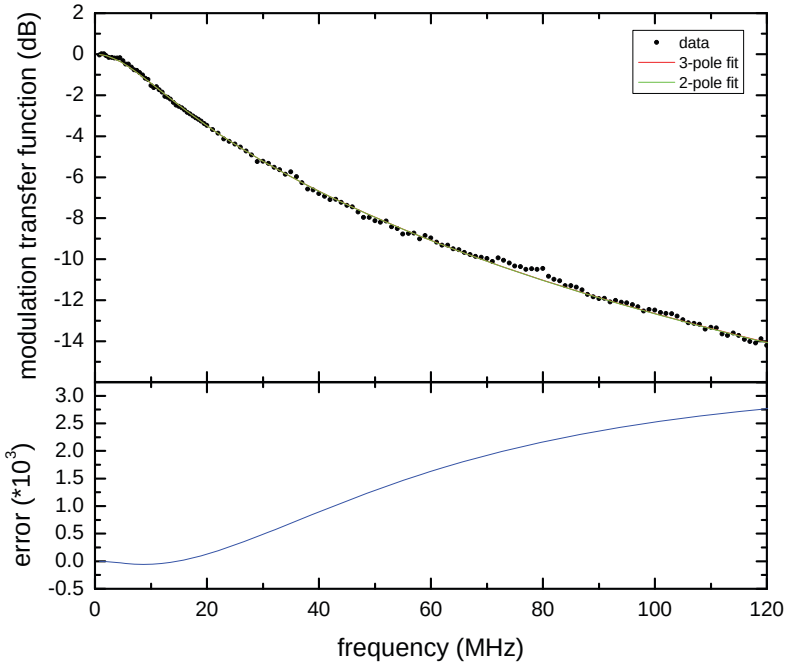

Figure 6. Example MTF data with fits from Equation 12 as well as the more typical two-pole function found in the literature. This indicates it may be sufficient to use the two-pole function for fitting.

barriers to the wells. A comparison of the fit of the data using the two-pole vs. the three-pole fit is shown in Figure 6 Using the two-pole produces significant differences in the extracted resonance frequency and damping constant.

4.5. Determining the differential gain

The resonance frequency of the laser is related to the differential gain of the laser according to:

$$\omega_r^2 \approx a\frac{v_g}{\tau_p}N_p, \tag{13}$$

where the differential gain is given by a . By plotting the resonance frequency data presented in Section 4.4 as a function of the photon density, the differential gain for each VECSEL cavity configuration was determined. The resonance frequencies and the fit to Equation 13 are provided in Figure 7. The values of the differential gain for the different configuration are presented in Table 2, which shows that the differential gain increases as the photon lifetime increases.

5. CONCLUSION

In this paper, we have analyzed a VECSEL and determined a series of operational parameters by examining the relevant laser rate equations. The rate equations describe the interaction of the carriers in the wells, the carriers

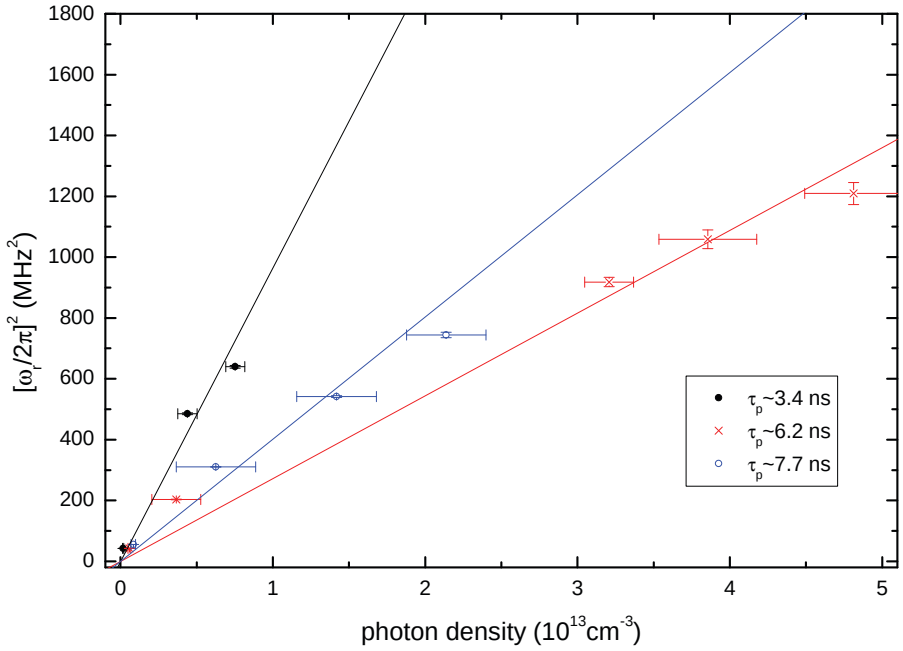

Figure 7. By plotting the resonance frequency as a function of photon lifetime and fitting the data to Equation 13, the differential gain of the VECSEL cavity can be determined.

in the barrier region and the photons in the cavity, under the assumption of a logarithmic dependence of the gain on the carrier density in the quantum wells. Examining these equations under steady state conditions provided an equation for the output power as a function of input power. By fitting this relationship to measurements of the laser threshold, we determined the transparency carrier density, the shift carrier density and the gain coefficient. Variations in the threshold data suggest that temperature effects are important. Our analysis of the rate equations yielded an expression for the slope efficiency; we used this relationship to fit experimental measurements of the slope efficiency and determined the optical scattering and the pump absorption of the cavity.

We also studied the VCSEL in the case of small signal modulation. The rate equations were examined by perturbing the carrier density, the photon density, the optical pumping and the gain with a first order Taylor expansion, we determined a mathematical expression for the MTF of the laser. We fitted this formula to experimental measurements of the MTF to extract the resonance frequency, the damping factor and the transition lifetime of the barriers to the well. A comparison of the resonance frequencies for different cavity configurations with different photon lifetimes enabled us to determine the differential gain.

REFERENCES

1. M. Kuznetsov, F. Hakimi, R. Sprague, and A. Mooradian, "Design and characteristics of high-power (>0.5-W CW) diode-pumped vertical-external-cavity surface-emitting semiconductor lasers with circular TEM_{00} beams," *IEEE J. of Sel. Top. in Quant. Elect.* **5**, pp. 561–573, May/June 1999.
2. A. Wójcik-Jedlińska, J. Muszalski, and M. Bugajski, "Photoluminescence studies of optical properties of VECSEL active region under high excitation conditions," in *J. Phys. Conf.*, *146*, p. 012031, 2009.
3. Y. Morozov, T. Leinonen, M. Morozov, S. Ranta, M. Saarinen, V. Popov, and M. Pessa, "Effect of pump reflections in vertical external cavity surface-emitting lasers," *New J. Phys.* **10**, p. 063028, 2008.

4. S. Chatterjee, W. Diehl, S. Horst, K. Hantke, W. W. Stolz, A. Thranhardt, S. W. Koch, P. Brick, M. Furitsch, S. Illek, I. Pietzonka, J. Luft, and W. W. Ruhle, "Nanosecond to microsecond dynamics of 1040 nm semiconductor disk lasers," in *Technical Digest Series, 2007 Quantum Electronics and Laser Science Conference, QELS*, p. 4431387, Institute of Electrical and Electronics Engineers Inc., (Piscataway, NJ 08855-1331, United States), 2007.
5. J. Hastie, S. Calvez, M. Dawson, T. Leinonen, A. Laakso, J. Lyytikinen, and M. Pessa, "High power CW red VECSEL with linearly polarized TEM_{00} output beam," *Opt. Exp.* **13**, pp. 77–81, 2005.
6. N. Hempler, J. Hopkins, M. Rattunde, B. Rosener, R. Moser, C. Manz, K. Kohler, J. Wagner, and D. Burns, "Tuning and brightness optimization of highperformance GaSb-based semiconductor disk lasers from 1.86 to 2.80μm," in *Euro. Conf. on Las. and Elect.-Opt*, p. 1, 2009.
7. L. Fan, T.-C. Hsu, M. Fallahi, J. Murray, R. Bedford, Y. Kaneda, J. Hader, A. Zakharian, J. Moloney, W. Stolz, and S. Koch, "Tunable watt-level blue-green vertical-external-cavity surface-emitting lasers by intracavity frequency doubling," *App. Phy. Lett.* **88**, pp. 251117–1 – 251117–3, June 2006.
8. D. Stothard, J. Hopkins, D. Burns, and M. Dunn, "Stable, continuous-wave, intracavity, optical parametric oscillator pumped by a semiconductor disk laser (VECSEL)," *Optics Express* **17**, pp. 10648–+, June 2009.
9. R. Häring, R. Paschotta, A. Aschwanden, E. Gini, F. Morier-Genoud, and U. Keller, "High-power passively mode-locked semiconductor lasers," *IEEE J. of Quant. Elect.* **38**, pp. 1268–1275, Sept. 2002.
10. L. Fan, M. Fallahi, J. Hader, A. R. Zakharian, M. Kolesik, J. V. Moloney, T. Qiu, A. Schülzgen, N. Peyghambarian, W. Stolz, S. W. Koch, and J. T. Murray, "Over 3 W high-efficiency vertical-external-cavity surface-emitting lasers and application as efficient fiber laser pump sources," *App. Phys. Lett.* **86**, p. 211116, 2005.
11. M. Waltonand N. Terry, J. Hader, J. Moloney, and R. Bedford, "Extraction of semiconductor microchip differential gain by use of optically pumped semiconductor laser," *Applied Physics Letters* **95**, pp. 111101–+, Sept. 2009.
12. J. Haderand J. Moloney and S. Koch, "Beyond the ABC: carrier recombination in semiconductor lasers," in *Society of Photo-Optical Instrumentation Engineers (SPIE) Conference Series*, M. Osinski, F. Henneberger, & Y. Arakawa, ed., *Presented at the Society of Photo-Optical Instrumentation Engineers (SPIE) Conference* **6115**, pp. 304–310, Mar. 2006.
13. L. Coldren and S. Corzine, *Diode Lasers and Photonic Integrated Circuits*, John Wiley & Sons, Inc., 1995.